Article **Journal Computer Technology**
June 2022, Vol.6 No.16 23-36

Energy curve and histogram thresholding implementation and evaluation with Aquila Cross-entropy optimization algorithm

Implementación y evaluación de umbrales de curvas de energía e histogramas con el algoritmo de optimización de entropía cruzada Aquila

ZARATE-NAVARRO, Omar†*, ROMO-GONZALEZ, Ana Eugenia, VILLALOBOS-ALONZO, María de los Ángeles and CABRERA-VILLASEÑOR, Héctor Ulises

Universidad Tecnológica de Jalisco, School of Engineering and Science, Information Technology Department, Guadalajara 44979, Mexico.

ID 1st Author: *Omar, Zarate-Navarro* / **ORC ID:** 0000-0002-2852-8822, **CVU CONACYT ID:** 335905

ID 1st Co-author: *Ana Eugenia, Romo-Gonzalez* / **ORC ID:** 0000-0002-4653-2593, **CVU CONACYT ID:** 212291

ID 2nd Co-author: *Maria de los Angeles, Villalobos-Alonzo* / **ORC ID:** 0000-0003-3052-8271, **CVU CONACYT ID:** 212718

ID 3rd Co-author: *Hector Ulises, Cabrera-Villaseñor* / **ORC ID:** 0000-0002-1165-219X

DOI: 10.35429/JCT.2022.16.6.23.36 Received: January 25, 2022; Accepted June 30, 2022

Abstract

This work proposes the implementation of minimum cross-entropy thresholding based on the aquila optimizer (MCE-AO) for the segmentation of base images and support to visually differentiate the different tissues present in the region. As an alternative to segmentation, the energy curve of the images was used, the energy curve has interesting properties, since it considers the spatial contextual information of each image and not only the intensity of the pixel as the histogram does, and in contrast to the histogram, the energy curve seems to be smoother by preserving the valleys and peaks. A comparison was made between the results calculated by the Aquila optimizer algorithm histograms of each image and the energy curve calculated for each image, showing considerable improvements in mean fitness. The quality of the segmented images was evaluated with the PSNR, SSIM and FSIM metrics, with the histogram and the energy curve, and a comparison of each of the results was made, showing improvement in the quality of the images segmented with the energy curve.

Aquila optimizer, Digital images segmentation, Energy curve

Resumen

En este trabajo se propone la implementación de la umbralización de entropía mínima cruzada basada en el optimizador de aquila (MCE-AO) para la segmentación de imágenes base y el apoyo para diferenciar visualmente los distintos tejidos presentes en la región. Como alternativa a la segmentación, se utilizó la curva de energía de las imágenes, la curva de energía tiene propiedades interesantes, ya que considera la información contextual espacial de cada imagen y no sólo la intensidad del píxel como lo hace el histograma, y en contraste con el histograma, la curva de energía parece ser más suave al preservar los valles y picos. Se realizó una comparación entre los resultados calculados por los histogramas del algoritmo optimizador Aquila de cada imagen y la curva de energía calculada para cada imagen, mostrando mejoras considerables en la aptitud media. La calidad de las imágenes segmentadas se evaluó con las métricas PSNR, SSIM y FSIM, con el histograma y la curva de energía, y se realizó una comparación de cada uno de los resultados, mostrando una mejora en la calidad de las imágenes segmentadas con la curva de energía.

Optimizador aquila, Segmentación de imágenes digitales, Curva de energía

Citation: ZARATE-NAVARRO, Omar, ROMO-GONZALEZ, Ana Eugenia, VILLALOBOS-ALONZO, María de los Ángeles and CABRERA-VILLASEÑOR, Héctor Ulises. Energy curve and histogram thresholding implementation and evaluation with Aquila Cross-entropy optimization algorithm. Journal Computer Technology. 2022. 6-16:23-36.

* Correspondence to the author (E-mail: ozarate@utj.edu.mx, avillalobos@utj.edu.mx).
† Researcher contributing as first author.

Introduction

This paper intends to check the efficiency of the Aquila optimization algo- rithm (AO) in comparison with other similar optimization algorithms, and to threshold several images with the help of the minimum cross-entropy calcula- tion (MCE), in a second phase it is intended to replace the histogram of each and every image by the energy curve and verify again the efficiency of the AO algorithm and the thresholding of the images.

Image segmentation provides important support for pre-processing tech- niques, as it allows the division of consistent, non-overlapping areas of the image, where specific attributes such as shape, intensity or texture are shared. Seg- mented brain magnetic resonance imaging has been extensively studied, taking into account that accurate segmentation can support the identification of dis- eases such as Alzheimer's, dementia or multiple sclerosis Simu & Lal (2017).

Image segmentation can be classified into thresholding techniques, clustering approaches, region methods and modelbased techniques Hinojosa et al. (2018) Hiralal & Menon (2016). Thresholding is a simple image segmentation method- ology yet powerful and efficient used to separate or distribute pixels into various regions on a given image by setting different thresholds values (th) along the intensity histogram. Thresholding is classified according to the number of th, as bilevel or multilevel (BTH and MTH, respectively). MTH consists of dividing the image using multiple threshold values to separate the image into several classes or thresholds. As the thresholds increase, so does the computational complexity, therefore, efficient selection on the number of thresholds is impor- tant Sezgin & Sankur (2004). Several studies have been proposed determining the optimal th values to implement. Such as the work proposed by Kittler and Illingworth Kittler Illingworth (1986) Kittler & Illingworth (1986), Abu-taleb (1989) Pal (1996) Otsu (1979).

Methods that have implemented entropy have been widely adopted by the image processing research community, as it has proven to be very efficient for image segmentation Oliva et al. (2019) Du et al. (2006), and is typically referred to as the minimum cross-entropy criterion (MCE) Li & Lee (1993). MCE can determine a set of thresholds by minimizing the cross-entropy from an image's histogram. However, MCE is only an entropic criterion, not a complete methodology for thresholding. MCE can support an exhaustive search and evaluation of possible combinations of thresholds, but this is impractical. However, to alleviate the computational burden, stochastic opti- mization algorithms (SOA) are often applied. SOAs rely on stochasticity to help their operatorsfind optimal solutions in reasonable times. Multiple approaches employing randomization are found in the literature. Some examples of SOAs applied to the multilevel thresholding of images in Khairuzzaman Chaudhury (2017) Khairuzzaman & Chaudhury (2017) Tang et al. (2011) Miller & Goldberg (1995) Avcibas et al. (2002) Liu et al. (2015).

Histogram-based thresholding is one of the most used approaches for image segmentation. There have been efforts to incorporate contextual informationinto the thresholding process. Some of the most relevant approaches incorporate the spatial information into the segmentation Ghosh et al. (2007). It was recently coupled with the Cuckoo Search algorithm Pare et al. (2016) and later extended with the use of a grey-level co-occurrence Pare et al. (2017). The Energy func- tion (EF) calculates the energy of each level and intensity of each pixel taking into account position and proximity. The EF generates the energy curve which has the same characteristics as the histogram. Each energy curve contains some peaks, and in this case, it can be separated according to a number of modes Pare et al. (2016). Therefore it is possible to find a threshold in a valley between two nodes Cheng et al. (2002). In related literature, the use of CS with EF was proposed to establish image segmentation Pare et al. (2016). Meanwhile, in [44], the segmentation approach using GA to find thresholds and printing with the energy curve is addressed in Patra et al. (2014).

Among the multilevel thresholding techniques, most of them focus on histogram-based thresholding which is very efficient for bilevel thresholding, however it is not fully effective for selecting the spatial contextual information of the images and determining the optimal thresholds.

Pare implements the cuckoo search (CS) and egg-laying radius cuckoo search (ELR-CS) optimization algorithms with different parameter analysis to solve the color image multilevel thresholding problem using the energy curve generated by the energy function Pare et al. (2016), Kandhway Srikanth & Bikshalu (2021), propouse the optimal thresholding based on spatial contextbased multilevel en- ergy curves for image segmentation using soft computing techniques Srikanth & Bikshalu (2021), Patra proposes the context-sensitive multilevel moralization for image segmentation by means of genetic algorithms Patra et al. (2014), in spite of the previous works, in the present work a direct comparison was made between the results of the thresholding of eleven base images by means of seven optimization algorithms, in the first instance based on the histogram of each image and later the energy curve of all the images was generated to make a direct comparison of all the results found with both spectra, noting the improvement of the results when using the energy curve.

In this paper we present the thresholding of images but replacing the his- togram by an energy function to determine the energy curve of each image, which takes into account the spatial contextual information of each image. To generate the optimal thresholding of each image, the histogram of the images is replaced by the energy curve generated for each of the images. Additionally we propose a novel method based on the Aquila Optimization algorithm AO in convination with minimum cross-entropy multi-level segmentation (MCE-AO) Abualigah et al. (2021a). The MCE-AO employs the cross-entropy as its fitness function and the AO capabilities to deal with multimodal functions to search for the optimal solution to the multi-level segmentation from histogram base images, the energy curve from base images is generated by the energy func- tion to search the best multi-level segmentation, an compare both results.

The Minimum Cross Entropy Aquila Optimization Algorithm (MCE-AO) presents competitive results in comparison with the optimization algorithms Sunflower Optimizer Yuan et al. (2020), Particle Swam Optimization Oliva et al. (2019), Differential Evolution Storn Price (1997) Storn & Price (1997), Houssein et al. (2020), Arithmetic Optimization Algorithm Abualigah et al. (2021a), Harmony Search Yang (2009) when implemented with 2,4,5,8,16 and 32 thresholds the results are presented, based on the mean fitness and standard deviation from each algorithm. Multilevel thresholding based on the histogram only takes into account the frequency of occurrence of a certain intensity level, but does not take into account all spatial information.

Taking contextual information into account can help to improve the quality of the segmentation of an image, since in this way not only the pixel value is taken into account, but also the proximity is taken into account. By taking the energy curve into account, the spatial information is brought to a curve with the same properties as the histogram. The same seven computational optimization algorithms were implemented as in the previous chapter, but instead of using the histogram, the energy curve of each of the base images was calculated and based on the energy curve, the mean fitness of each image and the standard deviation were obtained, where a considerable improvement can be observed in comparison with the histogram. We present the comparison of results between the implementation of the algorithms to the histograms of the base images and the results when implementing the algorithms to the energy curve of each of the base images, We can see that when implementing the energy curve to the algorithms the results of multilevel segmentation improves considerably.

Aquila optimizer

The Aquila Optimizer Algorithm (AO) simulates Aquila´s behavior during hunting in which showing the actions of each step of the hunt. AO algorithm are represented in four methods. Selecting the search space by high soar with the vertical stoop, exploring within a diverge search space by contour flight with short glide attack, exploiting within a converge search space by low flight with slow descent attack, and swooping by walk and grab prey Abualigah et al. (2021b).

The AO algorithm can transfer from exploration steps to exploitation steps using different behaviors based on this condition ift $\leq \left(\frac{2}{3}\right) \times T$

Expanded exploration X*1*

Aquila recognizes the prey area and selects the best hunting area by high soar with the vertical stoop. AO widely explore from high soar to determine the area of the search space, where the prey is. This behavior is mathematically presented as in Eq.1

$$X_1(t+1) = X_{best}(t) \times \left(1 - \frac{t}{T}\right) + (X_M(t) - X_{best}(t) * rand) \quad (1)$$

Where, X_1 $(t + 1)$ is the solution of the next iteration of t, which is generated by the first search method (X_1). X_{best} (t) is the best obtained solution until t_{th} iteration, this reflects the approximate place of the prey. This equation $\frac{1-t}{T}$) is used to control the expanded search (exploration) through the number of iterations. X_M (t) denotes to the locations mean value of the current solutions connected at t^{th} iteration, which is calculated using Eq. 2. rand is a random value between 0 and 1. t and T present the current iteration and the maximum number of iteration, respectively.

$$X_M(t) = \frac{1}{N}\sum_{i=1}^{N} X_i(t), \forall j = 1,2,\ldots,Dim \quad (2)$$

Where, *Dim* is the dimension size of the problem and N is the number of candidate solution (population size).

Narrowed exploration (X*2*)

When the prey area is found from a high soar, the Aquila circles above the target prey, prepares the land, and then attacks. AO narrowly explores the selected area of the target prey in preparation for the attack. Behavior is mathematically presented as in Eq. 3

$$X_2(t+1) = X_{best}(t) \times Levy(D) + X_R(t) + (y - x) * rand \quad (3)$$

Where X_2 $(t + 1)$ is the solution of the next iteration of t, which is generated by the second search method (X_2). D is the dimension space, and $Levy(D)$ is the levy flight distribution function, which is calculated using Eq. 4. $X_R(t)$ is a random solution taken in the range of $[1N]$ at the i^{th} iteration.

$$Levy(D) = s \times \frac{u \times \sigma}{|v|^{\frac{1}{\beta}}} \quad (4)$$

Where s is a constant value fixed to 0.01, u, and are random numbers between 0 and 1. σ is calculated using Eq. 5

$$\sigma = \left(\frac{\Gamma(1+\beta) \times sine\left(\frac{\pi\beta}{2}\right)}{\Gamma\left(\frac{1+\beta}{2} \times \beta \times 2\left(\frac{\beta-1}{2}\right)\right)}\right) \quad (5)$$

Where β is a constant value fixed to 1.5. In Eq. 1 y and x are used to present the spiral shape in the search, which are calculated as follows.

$$y = r \times cos(\Theta) \quad (6)$$

$$y = r \times sin(\Theta) \quad (7)$$

Where:

$$r = r_1 + U \times D_1 \quad (8)$$

$$\Theta = -\omega \times D_1 + \Theta_1 \quad (9)$$

$$\Theta 1 = \frac{3 \times \pi}{2} \quad (10)$$

r_1 takes a value between 1 and 20 for fixed the number of search cycles, and U is a small value fixed to 0.00565. D_1 is integer numbers from 1 to the length of the search space (*Dim*), and ω is a small value fixed to 0.005.

Expanded exploitation (X*3*)

The prey area is specified accurately, and the Aquila is ready for landing and attack, the Aquila descends vertically with a preliminary attack to discover the prey reaction. AO exploits the selected area of the target to get close of prey and attack. This behavior is mathematically presented as in Eq. 11.

$$X_3(t+1) = (X_{best}(t) - X_M(t)) \times \alpha - rand + ((UB - LB) \times rand + LB) \times \delta \quad (11)$$

Where $X_3(t+1)$ is the solution of the next iteration of t, which is generated by the third search method (X_3). $X_{best}(t)$ refers to the approximate location of the prey until i^{th} iteration (the best obtained solution), and $X_M(t)$ denotes to the mean value of the current solution at t^{th} iteration, which is calculated using Eq. 2. *rand* is a random value between 0 and 1. α and δ are the exploitation adjustment parameters fixed in this paper to a small value (0.1). LB denotes to the lower bound and UB denotes to the upper bound of the given problem.

Narrowed exploitation *(*X*4)*

Aquila got close to the prey, the Aquila attacks the prey over the land according to their stochastic movements. This method called walk and grab prey, AO attacks the prey in the last location. This behavior is mathematically presented as in Eq. 12.

$$X_4(t+1) = QF \times X_{best}(t) - (G_1 \times X(t) \times rand) - G_2 \times Levy(D) + rand \times G_1 \quad (12)$$

Where $X_4(t+1)$ is the solution of the next iteration of t, which is generated by the fourth search method (X_4) QF denotes to a quality function used to equilibrium the search strategies, which is calculated using Eq. 13. G_1 denotes various motions of the AO that are used to track the prey during the elope, which is generated using Eq. 14. G_2 presents decreasing values from 2 to 0, which denote the flight slope of the AO that is used to follow the prey during the elope from the first location (1) to the last location (t), which is generated using Eq. 15. $X_{(t)}$ is the current solution at the t^{th} iteration.

$$QF(t) = t^{\frac{2 \times rand - 1}{(1-T)^2}} \quad (13)$$

$$G_1 = 2 \times rand - 1 \quad (14)$$

$$G_2 = 2 \times \left(1 - \frac{t}{T}\right) \quad (15)$$

$QF_{(t)}$ is the quality function value at the t^{th} iteration, and rand is a random value between 0 and 1. t and T present the current iteration and the maximum number of iteration, respectively. $Levy(D)$ is the levy flight distribution function calculated using Eq. 4.

Image segmentation and minimum cross-entropy

The concept of entropy was propocesd by Kullback Kullback (1997) considering two probability distributions J = $\{j_1, j_2, ..., j_N\}$ and G = $\{g_1, g_2, ..., g_N\}$ of the same set; then, the information-theoretic distance measured between J and G is called cross entropy or divergence:

The basic idea of image thresholding is to select threshold values that would separate regions properly over an image. Statistic tools can be applied to clearly separate different classes over the shape of a distribution. One tool is the parametric criterion based on the cross-entropy Kullback (1997). Cross-entropy takes two distribution J = $\{j_1, j_2, ..., j_N\}$ and G = $\{g_1, g_2, ..., g_N\}$ over the same set and calculates

$$D(J, G) = \sum_{i=1}^{N} j_i \log \frac{j_i}{g_i} \quad (16)$$

Li and Lee Li & Lee (1993) took inspiration in the concept of cross-entropy from information theory, and they applied it into a binary segmentation problem. The Minimum Cross Entropy (MCET) problem takes the histogram from an image and divides it into subsets. Cross-entropy is calculated for those subsets. The objective was to find the best set of thresholds that minimize the cross-entropy of such partition. In the case of a grayscale 8-bit digital image, the pixel values range from 0 to 255, where the maximum value 255 is represented as L. Then, a threshold value th segments an image as

$$I_t(x, y) = \begin{cases} \mu(1, th), & I(x, y) < th, \\ \mu(th, L+1), & I(x, y) \geq th, \end{cases} \quad (17)$$

where

$$\mu(a, b) = \sum_{i=a}^{b-1} ih^{Gr}(i) / \sum_{i=a}^{b-1} h^{Gr}(i) \quad (18)$$

Expression can be rewritten in the form of an objective function:

$$f_{Cross}(th) = \sum_{i=1}^{th-1} ih^{Gr}(i) \log\left(\frac{i}{\mu(1,th)}\right) + \sum_{i=th}^{L} ih^{Gr}(i) \log\left(\frac{i}{\mu(th,L+1)}\right) \quad (19)$$

ISSN 2531-2197

The Minimum Cross Entropy was designed to address a single threshold value that partitions the histogram into two classes. Most scenes require more than two classes to segment the image properly. To address this issue, the MCET problem is transformed into a multilevel formulation as:

$$f_{Cross}(th) = \sum_{i=1}^{L} ih^{Gr}(i)\log(i) - \sum_{i=1}^{th-1} ih^{Gr}(i)\log\big(\mu(1,th)\big) - \sum_{i=th}^{L} ih^{Gr}(i)\log\big(\mu(th,L+1)\big) \quad (20)$$

Multilevel of the Minimum Cross Entropy, takes a set of *k* thresholds in the form of a vector th = $[th_1, th_2, ..., th_k]$.

$$f_{Cross}(\boldsymbol{th}) = \sum_{i=1}^{L} ih^{Gr}(i)\log(i) - \sum_{i=1}^{nt} H_i \quad (21)$$

Where q corresponds to the Entropies and thresholds to calculate.

$$H_1 = \sum_{i=1}^{th_1-1} ih^{Gr}(i)\log\big(\mu(1,th_1)\big) \quad (22)$$

$$H_q = \sum_{i=th_{q-1}}^{th_q-1} ih^{Gr}(i)\log\Big(\mu\big(th_{q-1},th_q\big)\Big), 1 < q < k \quad (23)$$

$$H_k = \sum_{i=th_k}^{L} ih^{G_r}(i)log\Big(\mu\big(th_q, L+1\big)\Big) \quad (24)$$

Several segmentation techniques are available as the results of decades of research. Among the developed techniques, the thresholding approach is the most simple, robust, and accurate of all of them Hammouche et al. (2010) Sezgin & Sankur (2004).

Minimum cross-entropy by AO

The proposed MCE-EC approach is described for the segmentation of digital base images from a data set of eleven. The key elments of the proposed algorithm are illustrated in the next subsections.

Problem formulation

The proposed approach takes a multilevel thresholding approach for segmentation, where a digital image is analyzed in terms of pixel intensity to partition the image's energy curve into a finite number of classes. The partition is defined as a set of threshold values along with the energy curve. The Aquila Optimizer (AO) is used to propose candidate configurations of segmentations, while the Minimum Cross-Entropy (MCE) criteria is used to determine if such arrangement is adequate.

MCE and AO work together to find optimal threshold values that can segment an image with results through an iterative process.

The minimum cross-entropy thresholding can be stated as an optimization problem given by

$$\text{Subjectto } \ \mathbf{th} \in \mathbf{X} \quad (25)$$

$$argmin_{th} \ f_{Cross}(\mathbf{th}) \quad (26)$$

Where corresponds to the MCE formulation of Eq 21. The set of restrictions for the feasible space is given by the possible intensity values of a pixel encoded in an 8-bit (0-255) representation $X = \{th \in R^n | 0 \leq th_j \leq 255, j = 1,2,...,n\}$

Encoding

In the context of stochastic optimization algorithms, the encoding used for the representation of a solution is important. In AO, the optimization start the improvement procedures by generating a random predefined set of candidate solutions, called population. Through the trajectory of repetition, the search strategies of the AO explore the reasonable positions of the near-optimal solution or the best obtained solution. Each solution updates its positions according to the best-obtained solution by the optimization processes of the AO. Finally, the search process of the AO is terminated when the end criterion is met.

Energy curve

Energy curve from an image provides an alternative to the histogram-based segmentation. Energy curve has alternative properties such as it considers spatial information of the image and not just the intensity of the pixel. As the histogram, energy curves seem to be smoother, preserving valleys and peaks. Image thresholding technique consists of search the corresponding threshold values in the middle of the valley regions from the energy curve. Every valley exists between two adjacent modes, and each mode characterizes an object present in the image. A digital image *I* used can be defined as a matrix $I = \{l_{ij}, 1 \leq i \leq m, 1 \leq j \leq n\}$ of size $m \times n$ where l_{ij} denotes the gray level of the image *I* at the pixel (i,j).

The maximum value of the gray intensity of the image I is denoted as L. A neighborhood N of order d at given position (i,j) is used $N_{ij}^{d} = \{(i+u, j+v), (u,v) \epsilon N^{d}\}$. Value of d determines the configuration that the neighborhood system takes Ghosh et al. (2007).

Recently, the energy curve was introduced to incorporate spatial information into the thresholding method Ghosh et al. (2007) Patra et al. (2014)

Accurate selection of thresholding values generates good segmentation results. The energy of the image I at gray intensity value I $(0 \leq l \leq L)$ is calculated by generating a two-dimensional matrix for every intensity value as $B_l = \{b_{i,j}, 1 \leq i \leq m, 1 \leq j \leq n\}$ where $b_{i,j} = 1$ if the intensity at the current position is greater than l the intensity value $(l_{i,j} > l)$, or else $b_{i,j} = -1$ Gray intensity value l is computed as:

$$E_l = -\sum_{i=1}^{m}\sum_{j=1}^{n}\sum_{pq\epsilon N_{ij}^{2}} b_{ij} \cdot b_{pq} + \sum_{i=1}^{m}\sum_{j=1}^{n}\sum_{pq\epsilon N_{ij}^{2}} C_{ij} \cdot C_{pq} \quad (26)$$

The right side of the equation Eq. 26 s a fixed term devoted to assuring a positive energy value $E_l \geq 0$. A quick look at Eq. 26 shows that for a given image I at intensity value l will be zero if all the elements of the binary image B_l are either 1 or 1. This approach determinates the energy associated to every intensity value of the image to generate a curve considering spatial contextual information of the image. Oliva et al. (2018)

(i-1, j-1)	(i-1, j)	(i-1, j+1)
(i, j-1)	(i, j)	(i, j+1)
(i+1, j-1)	(i+1, j)	(i+1, j+1)

Table 1 The spatial representation of the neighborhood system N^2

Experiments

This section presents the experiments conducted to appraise the effectiveness of the Aquila Optimizer and improvement of the thresholding performance by replacing the histogram of each image with the energy curveOliva et al. (2018).

First group of experiments examines the mean fitness and standard deviation results of the first experimental dataset that combines eleven well-known benchmark images (Cameraman, Lenna, Baboon, Man, Jet, Peppers, Living Room, Blonde, Walk Bridge, Butterfly and Lake) using the histogram from each image and after using energy curveOliva et al. (2018) of each base image.

These seven metaheuristic algorithms were selected to perform the experiments and apply it to eleven base images.

- Sunflower Optimization (SFO) Gomes et al. (2019) Yuan et al. (2020)
- Particle Swarm Optimization (PSO) Kennedy & Eberhart (1995) Maitra
- & Chatterjee (2008)
- Differential Evolution (DE) Storn & Price (1997) Cuevas et al. (2010)
- Levy Flight Distribution (LFD) Houssein et al. (2020)
- Arithmetic Optimization Algorithm (AOA) Abualigah et al. (2021a) Khatir et al. (2021)
- Harmony Search (HS) Yang (2009) Mahdavi et al. (2007)
- Aquila Optimizer (AO) Abualigah et al. (2021b)

All these optimization algorithms employ the Minimum Cross-Entropy (MCE) as the fitness functionLi & Lee (1993).

Experiments were performed with MATLAB R2018a at a 2.4 GHz Intel Core i5 CPU with a RAM memory of 12 GB.

Regarding the experiments, the threshold levels to search on each group of images are nt = 2, 3, 4, 5, 8, 16 and 32 values using minimum cross entropy function Li & Lee (1993) to segment base images. The reason these thresholds were chosen was because the performance of the algorithms is substantially affected as the number of thresholds increases, especially with 16 and 32 thresholds.

ISSN 2531-2197

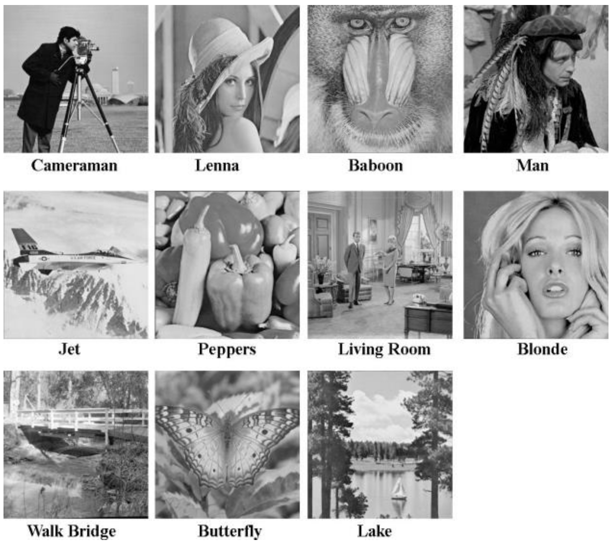

Figure 1 Eleven base image data set

Algorithm	Parameters	Value
Sunflower Optimization (SFO)	Number of Sunflowers	60
	Number of Experiments	30
	Pollination Values	0.05
	Mortality Rate, Best Values	0.1
	Survival Rate	1-(p+m)
	Iterations/Generations	1,000
Particle Swarm Optimization (PSO)	Social coefficient	2
	Cognitive coefficient	2
	Velocity clamp	2
	Maximum inertia value	0.2
	Minimum inertia value	0.9
Differential Evolution (DE)	Crossover Rate	0.5
	Number of Experiments	30
	Scale Factor	0.2
Levy Flight Distribution (LFD)	Max Iteration	1,000
	searchAgents no	35
Arithmetic Optimization Algorithm (AOA)	Materials Number	30
	Max Iteration	1,000
	Optimization functions	2, 6
Harmony Search (HS)	MaxAttempt	1,000
	Length of solution vector	20
	HM Accepting Rate	0.95
	Pitch Adjusting rate	0.4
Aquila Optimizer (AO)	Solution Number	30
	Max Iteration	1,000

Table 2 Parameters settings of the algorithms.

Results from metaheuristic algorithms from Base Images Histogram

In this subsection, the aforementioned optimization algorithms were implemented to threshold and generate the fitness mean and standard deviation of the eleven base images, each of the algorithms used the histogram from base images to generate mean fitness and Standard Deviation as results. It can be observed that the Aquila Optimizing Algorithm outperformed the other six algorithms on mean fitness. In the related literature, the search for the optimal threshold value focuses on a maximum of 5 levels, since an increment in the number of thresholds to search tends to raise the computational complexity for each test Rodriguez-Esparza et al. (2020).

Image		SFO		PSO		DE		LFD		AOA		HS		AO	
	nt	Mean	Std	Mean	Std	Mean	Std	Mean	Std	Mean	Std	Mean	Std	Mean	Std
Cameraman	2	1.4117	0.01096	1.6651	0.17473	1.8029	0.036123	1.4128	0.02026	1.4110	0.03672	1.4477	0.081087	**1.4018**	**0.0002**
	3	0.8469	0.06988	0.9549	0.07221	1.0170	0.087347	0.8109	0.05896	0.7978	0.07433	0.8745	0.141196	**0.7683**	**0.0058**
	4	0.6054	0.04051	0.8119	0.14055	0.7439	0.041957	**0.5814**	0.04232	0.6048	0.07148	0.5816	0.0419	0.5828	**0.0320**
	5	0.4578	0.03770	0.6349	0.09115	0.6161	0.07341	0.4660	0.05100	0.4754	0.08195	0.4449	0.04243	**0.4218**	**0.0170**
	8	0.2606	0.03200	0.3809	0.06041	0.3664	0.02945	0.2535	0.03074	0.2841	0.07683	0.2547	0.03730	**0.2364**	**0.0247**
	16	0.1025	0.01772	0.1524	0.02066	0.1571	0.02406	0.0986	0.01914	0.1600	0.05131	0.1113	0.01438	**0.0791**	**0.0115**
	32	0.0404	0.00601	0.0567	0.00783	0.0589	0.00774	0.0336	0.00614	0.1213	0.07454	0.0398	0.00498	**0.0263**	**0.0045**
Lenna	2	1.3773	0.01259	1.5693	0.14865	2.0904	0.018843	1.3709	0.00898	1.3684	0.00718	1.4117	0.051428	**1.3663**	**0.0000**
	3	0.8373	0.14342	0.9636	0.05595	1.1725	0.043313	0.7388	0.03397	0.7570	0.04682	0.7610	0.054975	**0.7183**	**0.0015**
	4	0.5989	0.08566	0.7460	0.10954	0.8508	0.047709	0.5057	0.03776	0.5174	0.03863	0.5256	0.062621	**0.4726**	**0.0047**
	5	0.4730	0.09972	0.6213	0.11400	0.6493	0.07692	0.3667	0.03571	0.3697	0.02475	0.3901	0.05983	**0.3318**	**0.0060**
	8	0.2775	0.04431	0.3437	0.05068	0.3879	0.04012	0.1979	0.02820	0.1958	0.03177	0.2333	0.04870	**0.1701**	**0.0119**
	16	0.1004	0.01243	0.1425	0.02351	0.1625	0.01876	0.0751	0.01103	0.0854	0.03324	0.1073	0.01446	**0.0563**	**0.0074**
	32	0.0354	0.00503	0.0526	0.00660	0.0576	0.00691	0.0246	0.00406	0.0491	0.02659	0.0404	0.00462	**0.0174**	**0.0018**
Baboon	2	1.2168	0.01205	1.3544	0.16955	1.3406	0.015671	1.2085	0.00705	1.2067	0.00527	1.2335	0.063511	**1.2051**	**0.0005**
	3	0.8669	0.11554	0.9427	0.07690	0.8646	0.053435	0.7604	0.02379	0.7566	0.01790	0.7963	0.070868	**0.7414**	**0.0013**
	4	0.6093	0.10167	0.7613	0.12657	0.6382	0.07473	0.5471	0.02870	0.5459	0.02616	0.5565	0.054813	**0.5119**	**0.0061**
	5	0.4853	0.07232	0.6102	0.08525	0.4888	0.04138	0.4129	0.03319	0.4035	0.02155	0.4149	0.03846	**0.3716**	**0.0059**
	8	0.2767	0.04355	0.3715	0.07544	0.2880	0.03291	0.2253	0.02273	0.2188	0.02986	0.2524	0.03568	**0.1969**	**0.0145**
	16	0.0978	0.01556	0.1478	0.02284	0.1199	0.01372	0.0828	0.01039	0.1050	0.03333	0.1087	0.01361	**0.0726**	**0.0099**
	32	0.0322	0.00674	0.0540	0.00655	0.0432	0.00454	0.0308	0.00558	0.0746	0.03964	0.0417	0.00496	**0.0234**	**0.0026**
Man	2	2.7579	0.01938	3.2564	0.52431	2.7639	0.056706	2.7419	0.01037	2.7367	0.00231	2.8214	0.114972	**2.7355**	**0.0002**
	3	1.8046	0.15348	2.0578	0.34861	1.7008	0.076341	1.6587	0.04704	1.6528	0.03271	1.6996	0.135738	**1.6234**	**0.0029**
	4	1.2426	0.16414	1.6754	0.28346	1.2238	0.185709	1.1314	0.11480	1.1270	0.16879	1.2176	0.144359	**1.0656**	**0.0428**
	5	0.9323	0.09134	1.0223	0.13226	0.9512	0.10419	0.8508	0.07648	0.8429	0.11535	0.9494	0.13691	**0.8129**	**0.0451**
	8	0.5177	0.05345	0.7609	0.14181	0.5861	0.07717	**0.4920**	0.06688	0.4957	0.08738	0.5736	0.09095	0.4935	0.0688
	16	0.2047	0.03880	0.3100	0.06165	0.2373	0.03906	**0.1816**	**0.02709**	0.2675	0.09267	0.2363	0.03691	0.2159	0.0373
	32	0.0733	0.01163	0.1244	0.02077	0.0937	0.01297	**0.0698**	0.01741	0.1704	0.10845	0.0898	0.01440	0.0741	0.0206
Jet	2	0.8261	0.00680	0.8803	0.04723	1.1744	0.012271	0.8214	0.00070	0.8231	0.00440	0.8287	0.009	**0.8209**	**0.0000**
	3	0.5408	0.03280	0.6280	0.08462	0.7362	0.020875	0.5190	0.01258	0.5246	0.01461	0.5223	0.014654	**0.5093**	**0.0016**
	4	0.3855	0.04167	0.4628	0.06827	0.5104	0.034301	0.3629	0.02753	0.3651	0.01713	0.3599	0.022906	**0.3385**	**0.0025**
	5	0.3032	0.04318	0.3740	0.05803	0.3987	0.03661	0.2779	0.03354	0.2647	0.01811	0.2721	0.03798	**0.2421**	**0.0124**
	8	0.1655	0.02981	0.2194	0.03520	0.2164	0.02063	0.1552	0.02787	0.1538	0.02887	0.1420	0.02595	**0.1277**	**0.0144**
	16	0.0680	0.00965	0.0891	0.01411	0.0846	0.00740	0.0564	0.01005	0.0873	0.04991	0.0612	0.00843	**0.0415**	**0.0056**
	32	0.0221	0.00335	0.0309	0.00483	0.0310	0.00262	0.0184	0.00415	0.0384	0.02241	0.0238	0.00246	**0.0133**	**0.0019**
Peppers	2	1.7490	0.02017	2.0570	0.27966	1.7507	0.02651	1.7514	0.03592	1.7362	0.00615	1.7827	0.094708	**1.7333**	**0.0002**
	3	1.2225	0.04887	1.4030	0.15742	1.2141	0.055776	1.1881	0.03040	1.1847	0.05880	1.1970	0.028188	**1.1624**	**0.0034**
	4	0.8439	0.10218	0.9587	0.07184	0.8553	0.124491	0.7951	0.06248	0.7849	0.05256	0.7972	0.080517	**0.7285**	**0.0122**
	5	0.6524	0.06552	0.8468	0.10640	0.6715	0.06556	0.6250	0.05798	0.6007	0.03045	0.6332	0.06993	**0.5554**	**0.0140**
	8	0.3488	0.03234	0.4765	0.07546	0.3855	0.04521	0.3375	0.04115	0.3559	0.06793	0.3572	0.04407	**0.2984**	**0.0282**
	16	0.1191	0.01599	0.2037	0.03138	0.1625	0.01691	0.1306	0.02048	0.2088	0.10511	0.1428	0.01652	**0.1132**	**0.0143**
	32	**0.0399**	**0.00540**	0.0701	0.00975	0.0561	0.00637	0.0441	0.00720	0.1215	0.06429	0.0514	0.00679	0.0414	0.0058
Image		SFO		PSO		DE		LFD		AOA		HS		AO	
Living Room	nt	Mean	Std	Mean	Std	Mean	Std	Mean	Std	Mean	Std	Mean	Std	Mean	Std
	2	1.8863	0.01391	2.0615	0.13908	1.8934	0.029966	1.8761	0.00906	1.8758	0.00592	1.9206	0.069879	**1.8736**	**0.0001**
	3	1.3089	0.09341	1.4043	0.17023	1.2133	0.040388	1.2124	0.04444	1.1855	0.01790	1.2182	0.084564	**1.1712**	**0.0025**
	4	0.8777	0.08782	0.9637	0.06581	0.8441	0.07446	0.8159	0.05771	0.8202	0.04460	0.8126	0.071433	**0.7616**	**0.0050**
	5	0.6526	0.06112	0.7911	0.10943	0.6560	0.06048	0.6017	0.04889	0.5913	0.03739	0.6214	0.08986	**0.5605**	**0.0265**
	8	0.3827	0.04906	0.4671	0.07450	0.3618	0.03683	0.3270	0.04366	0.3418	0.08413	0.3518	0.05181	**0.2814**	**0.0207**
	16	0.1450	0.02095	0.1800	0.02144	0.1458	0.01802	0.1240	0.02443	0.2052	0.10149	0.1358	0.01611	**0.1041**	**0.0154**
	32	0.0438	0.00603	0.0677	0.00827	0.0548	0.00662	0.0434	0.00631	0.1205	0.10874	0.0503	0.00557	**0.0397**	**0.0051**
Blonde	2	1.5260	0.00606	1.6165	0.07292	1.9460	0.041281	1.5303	0.02607	1.5206	0.00139	1.5991	0.071995	**1.5196**	**0.0003**
	3	0.8453	0.06209	0.9486	0.06697	1.0230	0.028807	0.8301	0.05209	0.8153	0.04567	0.8219	0.09166	**0.7829**	**0.0043**
	4	0.6174	0.06585	0.7670	0.11354	0.7390	0.056858	0.5962	0.04866	0.5980	0.05951	**0.5605**	0.055258	0.5654	**0.0374**
	5	0.4721	0.06131	0.6041	0.08157	0.5620	0.03376	0.4470	0.04945	0.4284	0.03609	0.4360	0.03942	**0.3953**	**0.0133**
	8	0.2609	0.03099	0.3293	0.06367	0.2911	0.03381	0.2284	0.04279	0.2517	0.07147	0.2317	0.03366	**0.2112**	**0.0237**
	16	0.0947	0.01182	0.1351	0.01792	0.1057	0.01057	**0.0798**	0.01303	0.1278	0.04503	0.0969	0.01390	0.0830	**0.0093**
	32	0.0343	0.00557	0.0487	0.00785	0.0374	**0.00434**	**0.0270**	0.00524	0.0943	0.05363	0.0358	0.00458	0.0318	0.0051
Walk Bridge	2	2.4590	0.01534	2.6081	0.15354	2.4595	0.021018	2.4532	0.04133	2.4465	0.01071	2.4920	0.085501	**2.4430**	**0.0001**
	3	1.6342	0.09068	1.7945	0.21712	1.5030	0.036119	1.5036	0.06055	1.5087	0.04649	1.5317	0.105859	**1.4703**	**0.0017**
	4	1.1647	0.07638	1.3004	0.12764	1.1007	0.067743	1.0581	0.03740	1.0602	0.02758	1.0661	0.051132	**1.0191**	**0.0070**
	5	0.9076	0.09779	0.9680	0.06440	0.8412	0.06239	0.8033	0.07663	0.7965	0.06484	0.7871	0.05790	**0.7418**	**0.0144**
	8	0.4764	0.06096	0.5923	0.09927	0.4668	0.04121	0.4261	0.04842	0.4183	0.04572	0.4318	0.05728	**0.3702**	**0.0313**
	16	0.1683	0.02217	0.2070	0.03383	0.1736	0.01663	0.1546	0.03317	0.2282	0.05674	0.1568	0.02784	**0.1416**	**0.0163**
	32	0.0517	0.00773	0.0684	0.00880	0.0600	0.00861	**0.0480**	0.00821	0.1611	0.08482	0.0499	**0.00617**	0.0486	0.0065
Butterfly	2	1.1879	0.01958	1.4027	0.22217	1.7714	0.014599	1.1766	0.00245	1.1752	0.00006	1.2016	0.030189	**1.1752**	**0.0001**
	3	0.7805	0.12572	0.8734	0.12416	1.0249	0.077505	0.6345	0.01597	0.6396	0.02285	0.6804	0.082018	**0.6234**	**0.0020**
	4	0.5489	0.08162	0.6900	0.13235	0.7238	0.055605	0.4419	0.03065	0.4429	0.03327	0.4746	0.057111	**0.4133**	**0.0020**
	5	0.4154	0.06613	0.5441	0.13045	0.5722	0.07480	0.3320	0.02593	0.3224	0.02082	0.3723	0.06380	**0.3042**	**0.0035**
	8	0.2535	0.02965	0.3345	0.07068	0.3248	0.04042	0.1768	0.01725	0.1738	0.02600	0.2299	0.04721	**0.1469**	**0.0116**
	16	0.1014	0.01845	0.1322	0.02140	0.1339	0.01636	0.0670	0.00837	0.0744	0.03371	0.1001	0.01548	**0.0482**	**0.0027**
	32	0.0347	0.00723	0.0530	0.00581	0.0495	0.00618	0.0221	0.00339	0.0310	0.01305	0.0403	0.00382	**0.0150**	**0.0014**
Lake	2	1.4479	0.01300	1.6250	0.13768	1.5808	0.024284	1.4405	0.00360	1.4416	0.00755	1.4863	0.105377	**1.4382**	**0.0000**
	3	1.0189	0.03851	0.9995	0.00187	1.0782	0.029962	0.9793	0.01692	0.9883	0.02917	0.9916	0.040038	**0.9627**	**0.0003**
	4	0.7319	0.06024	0.8416	0.10998	0.7722	0.056875	0.6948	0.03889	0.6920	0.05301	0.6815	0.059024	**0.6398**	**0.0124**
	5	0.5566	0.05256	0.7024	0.12129	0.5588	0.05048	0.5214	0.05763	0.4871	0.03074	0.4853	0.04585	**0.4490**	**0.0124**
	8	0.3018	0.04395	0.4203	0.07043	0.3286	0.03865	0.2683	0.04206	0.2849	0.09748	0.2607	0.03733	**0.2220**	**0.0140**
	16	0.1098	0.01976	0.1591	0.02422	0.1308	0.01341	0.0994	0.01670	0.1236	0.06509	0.1177	0.01813	**0.0755**	**0.0104**
	32	0.0384	0.00701	0.0559	0.00560	0.0474	0.00542	0.0338	0.00515	0.0626	0.02210	0.0441	0.00431	**0.0241**	**0.0038**

Table 3 Fitness mean and standard deviation implemented on base test images histogram

ISSN 2531-2197

Results from metaheuristic algorithms from Base Images Energy Curves

In this subsection, the aforementioned optimization algorithms were implemented to threshold and generate the fitness mean and standard deviation from the eleven base images, as same in the last chapter, but in this subsection were use the curve energy from each image to obtain and compare result as well with the histogram that is the common technique on this practice.

By using the energy curve to obtain the same data as with the histogram, we can observe that advantage of the Aquila Optimizing Algorithm prevails and even increases compared to the other algorithms results.

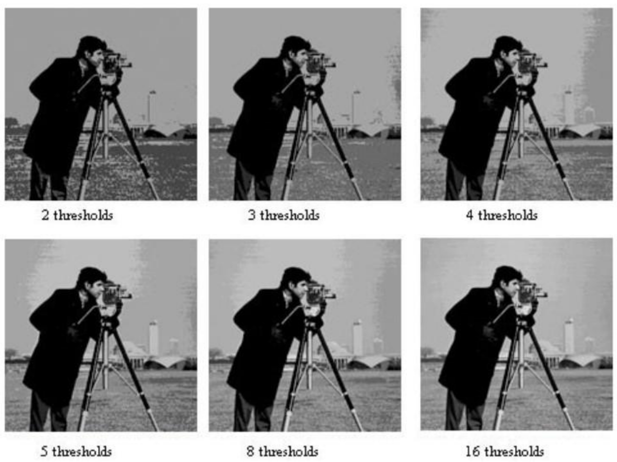

Figure 2 Camera Man segmented with AO 2,3,4,5,8 and 16 thresholds

Image		SFO		PSO		DE		LFD		AOA		HS		AO	
Cameraman	nt	Mean	Std	Mean	Std	Mean	Std	Mean	Std	Mean	Std	Mean	Std	Mean	Std
	2	0.7598	0.0015	0.8271	0.0585	0.7859	0.0498	0.7625	0.0074	0.7720	0.0418	0.8048	0.0765	**0.7582**	**0.0002**
	3	0.5441	0.0194	0.6075	0.0579	0.5549	0.0267	0.5365	0.0195	0.5383	0.0240	0.5563	0.0407	**0.5194**	**0.0148**
	4	0.3878	0.0376	0.4708	0.0724	0.4054	0.0395	0.3829	0.0328	0.3840	0.0391	0.4221	0.0605	**0.3424**	**0.0078**
	5	0.2808	0.0264	0.3628	0.0514	0.3067	0.0409	0.2752	0.0225	0.2834	0.0534	0.2903	0.0320	**0.2522**	**0.0090**
	8	0.1515	0.0259	0.1920	0.0332	0.1693	0.0225	0.1372	0.0218	0.1655	0.0746	0.1606	0.0273	**0.1189**	**0.0217**
	16	0.0572	0.0098	0.0758	0.0136	0.0686	0.0106	0.0478	0.0078	0.0726	0.0246	0.0664	0.0110	**0.0454**	**0.0071**
	32	0.0196	0.0034	0.0278	0.0030	0.0256	0.0031	0.0180	0.0030	0.0569	0.0253	0.0235	0.0029	**0.0157**	**0.0025**
Lenna	2	0.9984	0.0025	1.0000	0.0002	1.0143	0.0228	0.9991	0.0038	0.9978	0.0044	1.0622	0.0789	**0.9966**	**0.0000**
	3	0.5885	0.0807	0.7039	0.1539	0.5886	0.0763	0.5331	0.0401	0.5273	0.0147	0.5739	0.0824	**0.5110**	**0.0015**
	4	0.3862	0.0584	0.5385	0.1179	0.4260	0.0634	0.3433	0.0258	0.3442	0.0306	0.4153	0.0869	**0.3094**	**0.0032**
	5	0.3191	0.0476	0.4112	0.0833	0.3316	0.0518	0.2547	0.0189	0.2547	0.0164	0.3407	0.0806	**0.2347**	**0.0111**
	8	0.1736	0.0337	0.2313	0.0419	0.2051	0.0355	0.1319	0.0166	0.1461	0.0423	0.1931	0.0360	**0.1153**	**0.0079**
	16	0.0714	0.0142	0.0988	0.0185	0.0840	0.0105	0.0507	0.0081	0.0681	0.0325	0.0823	0.0129	**0.0397**	**0.0040**
	32	0.0238	0.0032	0.0329	0.0049	0.0311	0.0033	0.0167	0.0033	0.0347	0.0214	0.0302	0.0037	**0.0123**	**0.0014**
Baboon	2	0.6214	0.0025	0.7393	0.0982	0.6584	0.0450	0.6210	0.0031	0.6197	0.0010	0.6688	0.0428	**0.6194**	**0.0002**
	3	0.4628	0.0740	0.5534	0.0853	0.4437	0.0578	0.3973	0.0166	0.3878	0.0080	0.4384	0.0558	**0.3808**	**0.0003**
	4	0.3233	0.0565	0.4243	0.0786	0.3536	0.0673	0.2761	0.0110	0.2718	0.0091	0.3352	0.0470	**0.2627**	**0.0013**
	5	0.2789	0.0550	0.3327	0.0709	0.2862	0.0309	0.2102	0.0163	0.2039	0.0134	0.2698	0.0520	**0.1908**	**0.0049**
	8	0.1520	0.0224	0.2021	0.0376	0.1630	0.0278	0.1124	0.0104	0.1135	0.0218	0.1714	0.0318	**0.0982**	**0.0061**
	16	0.0593	0.0081	0.0804	0.0155	0.0733	0.0095	0.0406	0.0060	0.0533	0.0230	0.0745	0.0119	**0.0344**	**0.0032**
	32	0.0215	0.0039	0.0308	0.0053	0.0277	0.0039	0.0153	0.0030	0.0347	0.0227	0.0271	0.0033	**0.0111**	**0.0011**
Man	2	0.7819	0.0015	0.8530	0.0538	0.8105	0.0386	0.7824	0.0039	0.7814	0.0021	0.8353	0.0631	**0.7805**	**0.0000**
	3	0.5544	0.0544	0.6360	0.0824	0.5595	0.0525	0.5055	0.0160	0.5000	0.0109	0.5432	0.0452	**0.4926**	**0.0018**
	4	0.3771	0.0344	0.4884	0.0648	0.4186	0.0470	0.3652	0.0241	0.3516	0.0108	0.4269	0.0500	**0.3386**	**0.0062**
	5	0.2859	0.0194	0.3731	0.0406	0.3245	0.0410	0.2774	0.0240	0.2821	0.0311	0.3285	0.0500	**0.2548**	**0.0029**
	8	0.1545	0.0245	0.2183	0.0359	0.1870	0.0255	0.1442	0.0190	0.1520	0.0238	0.1874	0.0335	**0.1248**	**0.0133**
	16	0.0548	0.0088	0.0870	0.0135	0.0769	0.0090	0.0527	**0.0056**	0.0660	0.0158	0.0770	0.0098	**0.0455**	0.0071
	32	0.0189	0.0028	0.0295	0.0033	0.0278	0.0036	0.0174	0.0029	0.0419	0.0195	0.0259	0.0028	**0.0158**	**0.0019**
Jet	2	0.5711	0.0008	0.6217	0.0560	0.5876	0.0153	0.5716	0.0020	0.5712	0.0036	0.5898	0.0197	**0.5704**	**0.0000**
	3	0.4170	0.0384	0.4659	0.0546	0.4139	0.0256	0.3866	0.0186	0.3764	0.0106	0.4198	0.0459	**0.3683**	**0.0024**
	4	0.3201	0.0447	0.3504	0.0400	0.3165	0.0379	0.2804	0.0247	0.2679	0.0183	0.3169	0.0474	**0.2520**	**0.0088**
	5	0.2323	0.0325	0.2974	0.0582	0.2537	0.0316	0.2092	0.0188	0.2013	0.0158	0.2438	0.0399	**0.1926**	**0.0107**
	8	0.1401	0.0237	0.1754	0.0353	0.1499	0.0212	0.1169	0.0191	0.1110	0.0139	0.1353	0.0179	**0.1030**	**0.0127**
	16	0.0589	0.0079	0.0745	0.0136	0.0629	0.0100	0.0430	0.0075	0.0485	0.0134	0.0632	0.0085	**0.0376**	**0.0066**
	32	0.0205	0.0043	0.0263	0.0042	0.0245	0.0039	0.0141	0.0024	0.0317	0.0315	0.0238	0.0030	**0.0123**	**0.0020**
Peppers	2	1.1132	0.0020	1.1652	0.0470	1.1273	0.0177	1.1142	0.0038	1.1117	0.0007	1.1478	0.0331	**1.1114**	**0.0001**
	3	0.6409	0.0671	0.7984	0.1205	0.6616	0.0464	0.6211	0.0314	0.6247	0.0372	0.6968	0.0986	**0.5919**	**0.0015**
	4	0.4933	0.0613	0.6162	0.0837	0.5208	0.0588	0.4562	0.0247	0.4544	0.0384	0.5237	0.0708	**0.4249**	**0.0053**
	5	0.3773	0.0517	0.4806	0.0703	0.3978	0.0426	0.3379	0.0393	0.3171	0.0191	0.3762	0.0661	**0.2891**	**0.0073**
	8	0.2085	0.0318	0.2761	0.0423	0.2448	0.0400	0.1718	0.0180	0.1793	0.0385	0.2380	0.0362	**0.1582**	**0.0109**
	16	0.0779	0.0112	0.1202	0.0155	0.0966	0.0142	0.0686	0.0098	0.0894	0.0246	0.0945	0.0145	**0.0541**	**0.0097**
	32	0.0271	0.0052	0.0393	0.0048	0.0356	0.0053	0.0230	0.0032	0.0578	0.0327	0.0343	0.0045	**0.0174**	**0.0022**

Image		SFO		PSO		DE		LFD		AOA		HS		AO	
Living Room	nt	Mean	Std	Mean	Std	Mean	Std	Mean	Std	Mean	Std	Mean	Std	Mean	Std
	2	0.9392	0.0016	0.9817	0.0244	0.9679	0.0278	0.9424	0.0099	0.9376	0.0003	0.9955	0.0574	**0.9375**	**0.0000**
	3	0.6159	0.0708	0.7381	0.0955	0.6501	0.0814	0.5628	0.0134	0.5621	0.0135	0.6302	0.0703	**0.5503**	**0.0035**
	4	0.4679	0.0483	0.5526	0.0763	0.4708	0.0539	0.4007	0.0173	0.3970	0.0165	0.4583	0.0696	**0.3795**	**0.0049**
	5	0.3755	0.0469	0.4289	0.0587	0.3801	0.0605	0.2992	0.0221	0.2952	0.0190	0.3489	0.0544	**0.2743**	**0.0042**
	8	0.2188	0.0386	0.2490	0.0477	0.2149	0.0346	0.1566	0.0156	0.1610	0.0261	0.1948	0.0297	**0.1398**	**0.0094**
	16	0.0795	0.0131	0.1009	0.0173	0.0881	0.0100	0.0568	0.0101	0.0691	0.0199	0.0837	0.0115	**0.0491**	**0.0058**
	32	0.0266	0.0041	0.0341	0.0047	0.0319	0.0034	0.0208	0.0030	0.0511	0.0324	0.0305	0.0033	**0.0153**	**0.0017**
Blonde	2	0.5030	0.0018	0.6479	0.1186	0.5464	0.0772	0.5034	0.0049	0.5017	0.0019	0.5881	0.1078	**0.5006**	**0.0000**
	3	0.3926	0.0681	0.4765	0.1029	0.3753	0.0528	0.3072	0.0102	0.3029	0.0122	0.3827	0.0878	**0.2972**	**0.0012**
	4	0.3213	0.0593	0.3749	0.0662	0.2988	0.0487	0.2157	0.0080	0.2169	0.0139	0.2848	0.0423	**0.2076**	**0.0039**
	5	0.2504	0.0495	0.2954	0.0658	0.2429	0.0385	0.1654	0.0080	0.1668	0.0150	0.2343	0.0412	**0.1607**	**0.0062**
	8	0.1616	0.0334	0.1884	0.0375	0.1498	0.0254	0.0963	0.0111	0.0956	0.0067	0.1529	0.0248	**0.0873**	**0.0062**
	16	0.0660	0.0116	0.0799	0.0136	0.0672	0.0133	0.0380	0.0076	0.0440	0.0103	0.0699	0.0120	**0.0310**	**0.0026**
	32	0.0234	0.0044	0.0298	0.0038	0.0270	0.0040	0.0132	0.0024	0.0251	0.0144	0.0252	0.0030	**0.0106**	**0.0013**
Walk Bridge	2	1.2550	0.0027	1.3482	0.0980	1.2893	0.0381	1.2558	0.0060	1.2533	0.0015	1.3089	0.0660	**1.2527**	**0.0001**
	3	0.8517	0.0786	0.8966	0.0640	0.8170	0.0409	0.7692	0.0185	0.7675	0.0239	0.8045	0.0623	**0.7531**	**0.0023**
	4	0.6312	0.0707	0.6919	0.0954	0.5865	0.0633	0.5219	0.0396	0.5246	0.0331	0.5787	0.0646	**0.4832**	**0.0052**
	5	0.4696	0.0715	0.5183	0.0711	0.4651	0.0604	0.4092	0.0339	0.3842	0.0596	0.4369	0.0650	**0.3492**	**0.0135**
	8	0.2649	0.0434	0.2950	0.0402	0.2649	0.0380	0.2049	0.0244	0.2002	0.0300	0.2445	0.0326	**0.1752**	**0.0150**
	16	0.0937	0.0154	0.1073	0.0119	0.0953	0.0112	0.0785	0.0128	0.1008	0.0704	0.0938	0.0123	**0.0582**	**0.0049**
	32	0.0295	0.0042	0.0365	0.0047	0.0350	0.0039	0.0267	0.0041	0.0510	0.0287	0.0314	0.0034	**0.0179**	**0.0019**
Butterfly	2	0.7442	0.0019	0.9125	0.0757	0.7807	0.0439	0.7435	0.0028	0.7436	0.0043	0.8093	0.0688	**0.7420**	**0.0000**
	3	0.5102	0.0824	0.6340	0.1241	0.5112	0.0789	0.4245	0.0121	0.4226	0.0109	0.5050	0.1055	**0.4144**	**0.0003**
	4	0.3764	0.0714	0.4502	0.1141	0.3808	0.0491	0.3051	0.0188	0.2999	0.0095	0.3887	0.0739	**0.2899**	**0.0013**
	5	0.3029	0.0471	0.3715	0.0599	0.3236	0.0485	0.2254	0.0179	0.2212	0.0148	0.2958	0.0518	**0.2031**	**0.0063**
	8	0.1741	0.0282	0.2220	0.0390	0.1809	0.0296	0.1171	0.0141	0.1204	0.0160	0.1834	0.0367	**0.1002**	**0.0054**
	16	0.0674	0.0106	0.0953	0.0125	0.0815	0.0102	0.0449	0.0081	0.0563	0.0258	0.0772	0.0115	**0.0341**	**0.0028**
	32	0.0238	0.0040	0.0343	0.0052	0.0317	0.0042	0.0164	0.0028	0.0293	0.0201	0.0316	0.0046	**0.0110**	**0.0009**
Lake	2	1.0108	0.0008	1.0929	0.0797	1.0357	0.0242	1.0141	0.0073	1.0127	0.0075	1.0510	0.0413	**1.0101**	**0.0000**
	3	0.6004	0.0552	0.7318	0.0861	0.6066	0.0659	0.5711	0.0444	0.5747	0.0404	0.6316	0.1073	**0.5369**	**0.0045**
	4	0.4123	0.0623	0.5200	0.1007	0.4393	0.0605	0.3954	0.0391	0.3720	0.0226	0.4249	0.0533	**0.3505**	**0.0104**
	5	0.3219	0.0519	0.4112	0.0588	0.3580	0.0604	0.2892	0.0284	0.3098	0.0711	0.3342	0.0632	**0.2536**	**0.0128**
	8	0.1856	0.0308	0.2334	0.0284	0.2034	0.0358	0.1564	0.0197	0.1671	0.0551	0.1968	0.0360	**0.1362**	**0.0127**
	16	0.0690	0.0114	0.0968	0.0118	0.0832	0.0110	0.0597	0.0089	0.0923	0.0695	0.0770	0.0120	**0.0435**	**0.0060**
	32	0.0228	0.0039	0.0331	0.0043	0.0305	0.0038	0.0200	0.0025	0.0635	0.0554	0.0302	0.0031	**0.0146**	**0.0016**

Table 4 Fitness mean and standard deviation with base test images energy curve

ISSN 2531-2197

June 2022, Vol.6 No.16 23-36

	Cameraman				Lenna				Baboon			
	HISTOGRAM		ENERGY CURVE		HISTOGRAM		ENERGY CURVE		HISTOGRAM		ENERGY CURVE	
nt	Mean	Std	Mean	Std	Mean	Std	Mean	Std	Mean	Std	Mean	Std
2	1.4018	0.0002	0.7582	0.0002	1.3663	0.0000	0.9966	0.0000	1.2051	0.0005	0.6194	0.0002
3	0.7683	0.0058	0.5194	0.0148	0.7183	0.0015	0.5110	0.0015	0.7414	0.0013	0.3808	0.0003
4	0.5828	0.0320	0.3424	0.0078	0.4726	0.0047	0.3094	0.0032	0.5119	0.0061	0.2627	0.0013
5	0.4218	0.0170	0.2522	0.0090	0.3318	0.0060	0.2347	0.0111	0.3716	0.0059	0.1908	0.0049
8	0.2364	0.0247	0.1189	0.0217	0.1701	0.0119	0.1153	0.0079	0.1969	0.0145	0.0982	0.0061
16	0.0791	0.0115	0.0454	0.0071	0.0563	0.0074	0.0397	0.0040	0.0726	0.0099	0.0344	0.0032
32	0.0263	0.0045	0.0157	0.0025	0.0174	0.0018	0.0123	0.0014	0.0234	0.0026	0.0111	0.0011

	Man				Jet				Peppers			
	HISTOGRAM		ENERGY CURVE		HISTOGRAM		ENERGY CURVE		HISTOGRAM		ENERGY CURVE	
nt	Mean	Std	Mean	Std	Mean	Std	Mean	Std	Mean	Std	Mean	Std
2	2.7355	0.0002	0.7805	0.0000	0.8209	0.0000	0.5704	0.0000	1.7333	0.0002	1.1114	0.0001
3	1.6234	0.0029	0.4926	0.0018	0.5093	0.0016	0.3683	0.0024	1.1624	0.0034	0.5919	0.0015
4	1.0656	0.0428	0.3386	0.0062	0.3385	0.0025	0.2520	0.0088	0.7285	0.0122	0.4249	0.0053
5	0.8129	0.0451	0.2548	0.0029	0.2421	0.0124	0.1926	0.0107	0.5554	0.0140	0.2891	0.0073
8	0.4935	0.0688	0.1248	0.0133	0.1277	0.0144	0.1030	0.0127	0.2984	0.0282	0.1582	0.0109
16	0.2159	0.0373	0.0455	0.0071	0.0415	0.0056	0.0376	0.0066	0.1132	0.0143	0.0541	0.0097
32	0.0741	0.0206	0.0158	0.0019	0.0133	0.0019	0.0123	0.0020	0.0414	0.0058	0.0174	0.0022

	Living Room				Blonde				Walk Bridge			
	HISTOGRAM		ENERGY CURVE		HISTOGRAM		ENERGY CURVE		HISTOGRAM		ENERGY CURVE	
nt	Mean	Std	Mean	Std	Mean	Std	Mean	Std	Mean	Std	Mean	Std
2	1.8736	0.0001	0.9375	0.0000	1.5196	0.0003	0.5006	0.0000	2.4430	0.0001	1.2527	0.0001
3	1.1712	0.0025	0.5503	0.0035	0.7829	0.0043	0.2972	0.0012	1.4703	0.0017	0.7531	0.0023
4	0.7616	0.0050	0.3795	0.0049	0.5654	0.0374	0.2076	0.0039	1.0191	0.0070	0.4832	0.0052
5	0.5605	0.0265	0.2743	0.0042	0.3953	0.0133	0.1607	0.0062	0.7418	0.0144	0.3492	0.0135
8	0.2814	0.0207	0.1398	0.0094	0.2112	0.0237	0.0873	0.0062	0.3702	0.0313	0.1752	0.0150
16	0.1041	0.0154	0.0491	0.0058	0.0830	0.0093	0.0310	0.0026	0.1416	0.0163	0.0582	0.0049
32	0.0397	0.0051	0.0153	0.0017	0.0318	0.0051	0.0106	0.0013	0.0486	0.0065	0.0179	0.0019

	Butterfly				Lake			
	HISTOGRAM		ENERGY CURVE		HISTOGRAM		ENERGY CURVE	
nt	Mean	Std	Mean	Std	Mean	Std	Mean	Std
2	1.1752	0.0001	0.7420	0.0000	1.4382	0.0000	1.0101	0.0000
3	0.6234	0.0020	0.4144	0.0003	0.9627	0.0003	0.5369	0.0045
4	0.4133	0.0020	0.2899	0.0013	0.6398	0.0124	0.3505	0.0104
5	0.3042	0.0035	0.2031	0.0063	0.4490	0.0124	0.2536	0.0128
8	0.1469	0.0116	0.1002	0.0054	0.2220	0.0140	0.1362	0.0127
16	0.0482	0.0027	0.0341	0.0028	0.0755	0.0104	0.0435	0.0060
32	0.0150	0.0014	0.0110	0.0009	0.0241	0.0038	0.0146	0.0016

Table 5 Fitness mean and standard deviation with base test images histogram vs energy curve

Evaluating image quality

The quality of an image after being processed can be evaluated objectively and subjectively. The objective analysis involves numerical measures with or without references, with the reference being often called ground truth. Many approaches use no-reference quality metrics such as PSNR, SSIM, and FSIM.

PSNR

The Peak Signal to Noise Ratio (PSNR) estimates the ratio of distortion noise that occurs over a power signal Avcibas et al. (2002). PSNR is typically used to assess the quality of an image after being processed; it works by taking the original image and comparing its processed (distorted) counterpart on a logarithmic scale. A higher PSNR value indicates higher quality. The PSNR is computed as follows:

$$PSNR = 20log_{10}\left(\frac{255}{RMSE}\right), (dB) \tag{27}$$

$$MSE = \sqrt{\frac{\sum_{i=1}^{ro}\sum_{j=1}^{co}(I_{Gr}(i,j)-I_{th}(i,j))}{ro \times co}} \tag{28}$$

SSIM

The Structural Similarity Index Method (SSIM) is also a no-reference quality metric such as the PSNR. SSIM takes the concept of human perception into account. Image distortion is modeled after changes in structural information Wang et al. (2004). The structures considered are the luminance, contrast, and structure in the form of correlation between the original image and the modified version. The SSIM value goes from 0 to 1, where a higher SSIM value indicates higher quality. The SSIM is calculated using the next equations:

$$SSIM\ (I_{Gr}, I_{th}) = \frac{(2\mu_{I_{Gr}}\mu_{I_{th}} + C1)(2\sigma_{I_{Gr}}\sigma_{I_{th}} + C2)}{(\mu_{I_{Gr}}^2 + \mu_{I_{th}}^2 + C1)\ (\sigma_{I_{Gr}}^2 + \sigma_{I_{th}}^2 + C2)} \tag{29}$$

$$\sigma_{I_0 I_{Gr}} = \frac{1}{N-1}\sum_{i=1}^{N}(I_{Gr_i} + \mu_{Gr})(I_{th_i} + \mu_{I_{th}}) \tag{30}$$

Where μ_{IGr} and μ_{Ith} are the mean value of the original and the umbralized image respectively, for each image the values of σ_{IGr} and $\sigma_I th$ corresponds to the standard deviation. C1 and C2 are constants used to avoid the instability when $\mu_{I_{Gr}}^2 + \mu_{I_{th}}^2 \approx 0$, experimentally in both values are C1=C2=0.065.

FSIM

The Feature Similarity Index Method (FSIM) compares the original image against the processed one by considering features present on an image. A feature is a region of an image that contains interesting properties. Some examples of features are edges and corners. Since features are essential to understanding what is represented in an image. The FSIM works by finding features using two traditional methods; phase congruency (*PC*) and gradient magnitude (*GM*) Zhang et al. (2011). The FSIM value goes from 0 to 1, where a higher FSIM value indicates higher quality. The FSIM is obtained by:

$$FSIM = \frac{\sum_{w\in\Omega} S_L(w)PC_m(w)}{\sum_{w\in\Omega} PC_m(w)} \tag{31}$$

where Ω denotes the domain of the image

$$S_L(w) = S_{PC}(w)S_G(w) \tag{32}$$

ISSN 2531-2197

$$S_G(w) = \frac{2G_1(w)G_2(w)+T_2}{G_1^2(w)+G_2^2(w)+T_2} \quad (33)$$

$$G = \sqrt{G_x^2 + G_y^2} \quad (34)$$

$$PC(w) = \frac{E(w)}{(\varepsilon+\sum_n A_n(w))} \quad (35)$$

Segmentation quality

The information in the table 4 indicates that AO algorithm outperforms its counterparts in terms of fitness function with base images. However, in this type of work, an evaluation not associated with fitness performance is required. Segmented image quality is assessed by using the three non-reference metrics described, PSNR (Peak Signal to Noise Ratio), SSIM (Structural Similarity Index Method) and FSIM (Feature Similarity Index Method). In the above three metrics, a high value indicates a higher quality segmentation. Figure 3 shows a graphical comparison of the PSNR value of Brain MRI, with each of the counterpart algorithms of the tests represented as seven groups along the horizontal axis. In each group, the mean PSNR value was taken for all MRIs considering thirty runs for each of the algorithms and for each given number of thresholds (color-coded). The AO algorithm outperforms the other approaches at all thresholds considered.

Figure 4 shows the graphical comparison from the PSNR value of the base images, but in this case comparison is of the data obtained with the energy curve and in contrast with the data obtained from the traditional histogram, where as in the previous graph, thirty runs of each algorithm were taken for all the mean values of PSNR. It is possible to observe the superiority in quality when the values of the energy curve were taken.The graphical comparison in the Fig. 4, 6 and 8 show the better metrics from AO algorithm when using the energy curve versus the histogram of the base images.

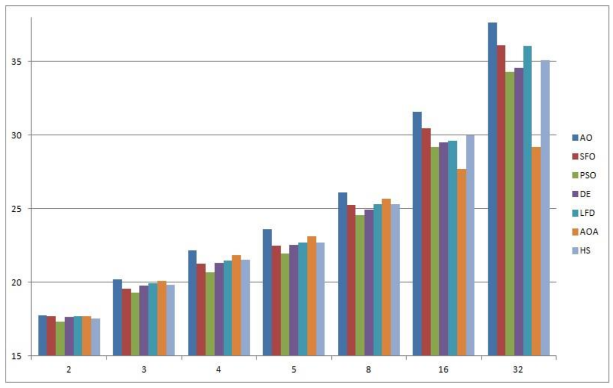

Figure 3 Comparative Algorithms PSNR Energy Curve

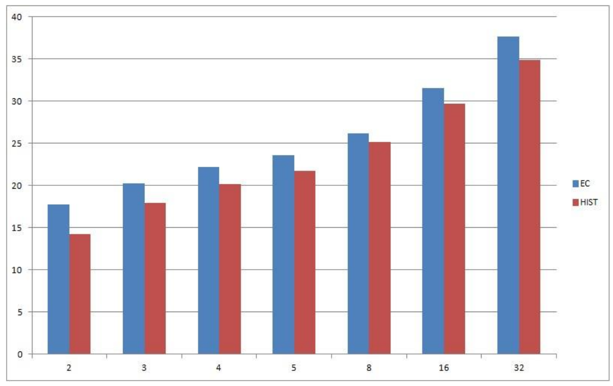

Figure 4 Comparative AO PSNR Energy Curve vs Histogram

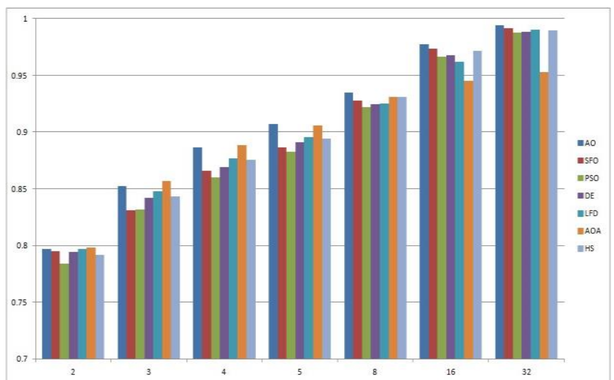

Figure 5 Comparative Algorithms SSINV Energy Curve

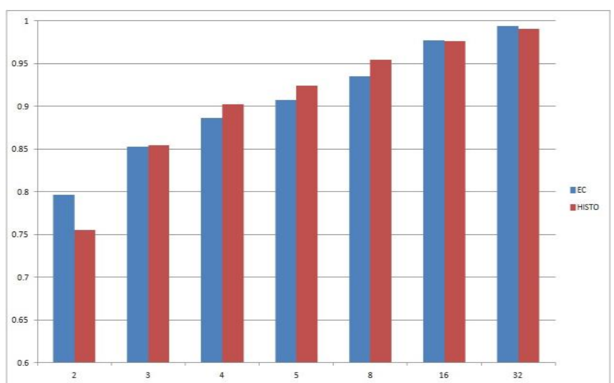

Figure 6 Comparative AO SSIMV Energy Curve vs Histogram

ISSN 2531-2197

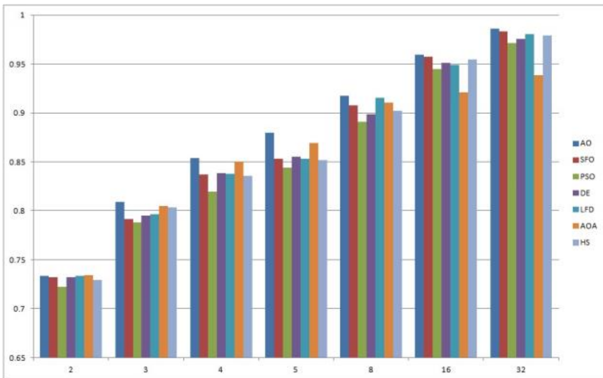

Figure 7 Comparative Algorithms FSIMV Energy Curve

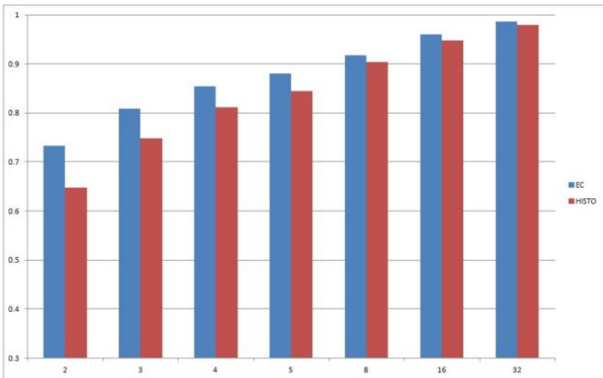

Figure 8 Comparative AO FSIMV Energy Curve vs Histogram

Conclusions

This paper presents a new MCE-AO approach designed to identify an optimal set of threshold values based on the energy curve of each of the baseline images and to properly segment them. The approach is based on the stochastic optimization algorithm called the aquila optimizer (AO) using minimum crossentropy as a nonparametric criterion.

The relevance of the MCE-AO is evaluated by and designed to determine whether the AO works well for general purpose image segmentation by using and comparing the results generated from each image histogram and energy curve. The proposed MCE-AO was compared with other stochastic optimization variants, namely the Sunflower Optimization Algorithm (SFO), Particle Swarm Optimization (PSO), Differential Evolution (DE), Levy Flight Distribution (LFD), Arithmetic Optimization Algorithm (AOA) and Harmony Search (HS). The proposed approaches were analyzed in terms of statistical significance with a post hoc test.

The segmentation quality of images was analyzed using relevant objective quality metrics, such as peak signal-to-noise ratio (PSNR), structural similarity index measure (SSIM), and feature similarity index. The MCE-AO provided robust results indicating its suitability for the task in terms of objective quality metrics. The MCE-AO was able to provide competitive and stable results compared to the other SOAs. In future work, the thresholding process could benefit from the inclusion of multidimensional Medical Magnetic Resonance Image information.

References

Abualigah, L., Diabat, A., Mirjalili, S., Abd Elaziz, M., & Gandomi, A. H. (2021a). The arithmetic optimization algorithm. *Computer methods in applied mechanics and engineering*, *376*, 113609.

Abualigah, L., Yousri, D., Abd Elaziz, M., Ewees, A. A., Al-qaness, M. A., & Gandomi, A. H. (2021b). Aquila optimizer: A novel meta-heuristic optimization algorithm. *Computers & Industrial Engineering*, *157*, 107250.

Abutaleb, A. S. (1989). Automatic thresholding of gray-level pictures using twodimensional entropy. *Computer vision, graphics, and image processing*, *47*, 22–32.

Avcibas, I., Sankur, B., & Sayood, K. (2002). Statistical evaluation of image quality measures. *Journal of Electronic imaging*, *11*, 206–223.

Cheng, H.-D., Jiang, X., & Wang, J. (2002). Color image segmentation based on homogram thresholding and region merging. *Pattern recognition*, *35*,373–393.

Cuevas, E., Zaldivar, D., & P´erez-Cisneros, M. (2010). A novel multi-threshold segmentation approach based on differential evolution optimization. *Expert Systems with Applications*, *37*, 5265–5271.

Du, Y., Wang, J., Guo, S.-M., Thouin, P. et al. (2006). Survey and comparative analysis of entropy and relative entropy thresholding techniques. *IEE Proceedings-Vision, Image and Signal Processing*, *153*, 837–850.

Ghosh, S., Bruzzone, L., Patra, S., Bovolo, F., & Ghosh, A. (2007). A contextsensitive technique for unsupervised change detection based on hopfieldtype neural networks. *IEEE Transactions on Geoscience and Remote Sensing*, *45*, 778–789.

Gomes, G. F., da Cunha, S. S., & Ancelotti, A. C. (2019). A sunflower optimization (sfo) algorithm applied to damage identification on laminated composite plates. *Engineering with Computers*, *35*, 619–626.

Hammouche, K., Diaf, M., & Siarry, P. (2010). A comparative study of various meta-heuristic techniques applied to the multilevel thresholding problem. *Engineering Applications of Artificial Intelligence*, *23*, 676–688.

Hinojosa, S., Pajares, G., Cuevas, E., & Ortega-Sanchez, N. (2018). Thermal image segmentation using evolutionary computation techniques. In *Advances in Soft Computing and Machine Learning in Image Processing* (pp. 63–88). Springer.

Hiralal, R., & Menon, H. P. (2016). A survey of brain mri image segmentation methods and the issues involved. In *The International Symposium on Intelligent Systems Technologies and Applications* (pp. 245–259). Springer.

Houssein, E. H., Saad, M. R., Hashim, F. A., Shaban, H., & Hassaballah, M. (2020). L´evy flight distribution: A new metaheuristic algorithm for solving engineering optimization problems. *Engineering Applications of Artificial Intelligence*, *94*, 103731.

Kennedy, J., & Eberhart, R. (1995). Particle swarm optimization. In *Proceedings of ICNN'95-international conference on neural networks* (pp. 1942–1948). IEEE volume 4.

Khairuzzaman, A. K. M., & Chaudhury, S. (2017). Multilevel thresholding using grey wolf optimizer for image segmentation. *Expert Systems with Applications*, *86*, 64–76.

Khatir, S., Tiachacht, S., Le Thanh, C., Ghandourah, E., Mirjalili, S., & Wahab, M. A. (2021). An improved artificial neural network using arithmetic optimization algorithm for damage assessment in fgm composite plates. *Composite Structures*, *273*, 114287.

Kittler, J., & Illingworth, J. (1986). Minimum error thresholding. *Pattern recognition*, *19*, 41–47.

Kullback, S. (1997). *Information theory and statistics*. Courier Corporation.

Li, C. H., & Lee, C. (1993). Minimum cross entropy thresholding. *Pattern recognition*, *26*, 617–625.

Liu, Y., Mu, C., Kou, W., & Liu, J. (2015). Modified particle swarm optimization-based multilevel thresholding for image segmentation. *Soft computing*, *19*, 1311–1327.

Mahdavi, M., Fesanghary, M., & Damangir, E. (2007). An improved harmony search algorithm for solving optimization problems. *Applied mathematics and computation*, *188*, 1567–1579.

Maitra, M., & Chatterjee, A. (2008). A hybrid cooperative–comprehensive learning based pso algorithm for image segmentation using multilevel thresholding. *Expert Systems with Applications*, *34*, 1341–1350.

Miller, B. L., & Goldberg, D. E. (1995). Genetic algorithms, selection schemes, and the varying e ects of noise. *Evolutionary Computation*, *4*, 113.

Oliva, D., Hinojosa, S., Abd Elaziz, M., & Ortega-S´anchez, N. (2018). Context based image segmentation using antlion optimization and sine cosine algorithm. *Multimedia Tools and Applications*, *77*, 25761–25797.

Oliva, D., Nag, S., Abd Elaziz, M., Sarkar, U., & Hinojosa, S. (2019). Multilevel thresholding by fuzzy type ii sets using evolutionary algorithms. *Swarm and Evolutionary Computation*, *51*, 100591.

Otsu, N. (1979). A threshold selection method from gray-level histograms. *IEEE transactions on systems, man, and cybernetics*, *9*, 62–66.

Pal, N. R. (1996). On minimum cross-entropy thresholding. *Pattern Recognition*, *29*, 575–580.

Pare, S., Bhandari, A. K., Kumar, A., & Singh, G. K. (2017). An optimalcolor image multilevel thresholding technique using grey-level co-occurrence matrix. *Expert Systems with Applications*, *87*, 335–362.

Pare, S., Kumar, A., Bajaj, V., & Singh, G. K. (2016). A multilevel color image segmentation technique based on cuckoo search algorithm and energy curve. *Applied soft computing*, *47*, 76–102.

Patra, S., Gautam, R., & Singla, A. (2014). A novel context sensitive multilevel thresholding for image segmentation. *Applied soft computing*, *23*, 122–127.

Rodriguez-Esparza, E., Zanella-Calzada, L. A., Oliva, D., Heidari, A. A., Zaldivar, D., P´erez-Cisneros, M., & Foong, L. K. (2020). An efficient harris hawks-inspired image segmentation method. *Expert Systems with Applications*, *155*, 113428.

Sezgin, M., & Sankur, B. (2004). Survey over image thresholding techniques and quantitative performance evaluation. *Journal of Electronic imaging*, *13*, 146–165.

Simu, S., & Lal, S. (2017). A study about evolutionary and non-evolutionary segmentation techniques on hand radiographs for bone age assessment. *Biomedical Signal Processing and Control*, *33*, 220–235.

Srikanth, R., & Bikshalu, K. (2021). Multilevel thresholding image segmentation based on energy curve with harmony search algorithm. *Ain Shams Engineering Journal*, *12*, 1–20.

Storn, R., & Price, K. (1997). Differential evolution–a simple and efficient heuristic for global optimization over continuous spaces. *Journal of global optimization*, *11*, 341–359.

Tang, K., Yuan, X., Sun, T., Yang, J., & Gao, S. (2011). An improved scheme for minimum cross entropy threshold selection based on genetic algorithm. *Knowledge-Based Systems*, *24*, 1131–1138.

Wang, Z., Bovik, A. C., Sheikh, H. R., & Simoncelli, E. P. (2004). Image quality assessment: from error visibility to structural similarity. *IEEE transactions on image processing*, *13*, 600–612.

Yang, X.-S. (2009). Harmony search as a metaheuristic algorithm. In *Musicinspired harmony search algorithm* (pp. 1–14). Springer.

Yuan, Z., Wang, W., Wang, H., & Razmjooy, N. (2020). A new technique for optimal estimation of the circuit-based pemfcs using developed sunflower optimization algorithm. *Energy Reports*, *6*, 662–671.

Zhang, L., Zhang, L., Mou, X., & Zhang, D. (2011). Fsim: A feature similarity index for image quality assessment. *IEEE transactions on Image Processing*, *20*, 2378–2386.

ISSN 2531-2197